Available online at www.sciencedirect.com
ScienceDirect
Journal of the European Ceramic Society 27 (2007) 1365–1371
www.elsevier.com/locate/jeurceramsoc

Mechanical properties and thermal shock behaviour of an alumina/zirconia functionally graded material prepared by electrophoretic deposition

Pavol Hvizdoš [a,*], Daniel Jonsson [a], Marc Anglada [a], Guy Anné [b], Omer Van Der Biest [b]

[a] *Universitat Politecnica de Catalunya, ETSEIB, Diagonal 647, 08028-Barcelona, Spain*
[b] *Department of Metallurgy and Materials Engineering, Katholieke Universiteit Leuven, Kasteelpark Arenberg 44, 3001 Heverlee, Belgium*

Available online 9 June 2006

Abstract

Mechanical properties of a symmetrical planar functionally graded material (FGM) of Al_2O_3 + 10% ZrO_2/Al_2O_3 + 30% ZrO_2/Al_2O_3 + 10% ZrO_2 prepared by electrophoretic deposition (EPD) and pressureless sintering were studied. Hardness and fracture toughness were measured using indentation methods on cross sections of samples. From the difference between lengths of cracks parallel and perpendicular to layers the residual stresses (arisen due to the thermal expansion coefficient mismatch) were calculated. Thermal shock resistance of particular layers was studied using indentation-quench method. The results were compared to those obtained from a reference non-layered composite material, prepared by the same fabrication technique.

Keywords: Al_2O_3; ZrO_2; Mechanical properties; Functionally graded materials; Thermal shock resistance

1. Introduction

The problem of the sensitivity to flaws in ceramics, which originates from its inherent brittleness and results in the unreliability in strength, has lead to the development of techniques to hinder these cracks to grow, and, as a result, an increase in strength. One common strategy is to introduce toughening mechanisms using platelets, secondary particles, whiskers or fibres. Another well recognised method that has proven inexpensive, and is commonly used in glasses, is the introduction of surface compressive stresses. In ceramics this can be obtained by forming a laminate ceramic composite. In multilayered materials with strong interfaces the difference in the thermal expansion coefficients between dissimilar materials generate thermal residual stresses during subsequent cooling.[1,2] The relative thickness of different layers determines the relative magnitudes of stresses, while the magnitude of the strain mismatch between the layers implies the absolute values of the residual stresses. However, abrupt transitions in the composition and properties of these materials often result in sharp local concentrations of stress, whether the stress is internal or applied externally. This may lead to cracking of the interface during cooling from the processing temperature or to delamination in service. A possible solution is a concept of functionally graded materials (FGMs). By definition FGMs are used to produce components featuring engineered gradual transitions in microstructure and/or composition, the presence of which is motivated by functional performance requirements that vary with the location within the part. With functionally graded materials, these requirements are met in a manner that optimises the overall performance of the component.[2] Their main feature is gradient in composition and/or phase distribution and related mechanical and physical properties. According to Suresh,[3] grading the interface between two dissimilar solids can be an attractive choice if bonding of thick layers (typically >1 mm) is required. Such controlled modifications of the composition can reduce the magnitude of the thermal stresses, suppress the plastic flow and cracking and improve interfacial bonding, provided that the graded microstructure is thermally stable during subsequent thermomechanical loading.

One of the techniques to produce planar FGMs is electrophoretic deposition (EPD) which allows to form a continuous compositional gradient by controlling the powder composition in the suspension from which particles are deposited on one of

* Corresponding author. Tel.: +34 93 4054454; fax: +34 93 4016706.
E-mail address: hvizdosp@yahoo.com (P. Hvizdoš).

0955-2219/$ – see front matter © 2006 Elsevier Ltd. All rights reserved.
doi:10.1016/j.jeurceramsoc.2006.05.030

the electrodes.[4] It is a fairly rapid and low cost process which leads to a close packed powder compact that needs sintering to achieve fully dense material components.

The aim of the present work is the study of microstructure and mechanical properties of alumina/zirconia functionally graded material prepared by electrophoretic deposition. Hardness, fracture toughness and residual stresses were measured by indentation methods. The finite element analysis and a simple layered model were also used to calculate the residual stress profiles. Ceramic materials, as candidates for use in thermal barrier coatings and in aerospace applications, would be subjected to steep thermal gradients and/or rapid temperature changes. Therefore, here it has been studied the crack extension induced by thermal shocks. The results were compared to those obtained by the same tests carried out on a reference homogeneous alumina/zirconia composite material.

2. Material

The material was an experimental grade manufactured by Katholieke Universiteit Leuven, Belgium. Its preparation had been described previously.[4] The starting materials were commercially available powders of 3 mol.% Y_2O_3 co-precipitated ZrO_2 (Daiichi grade HSY-3U) with an average particle size ~0.3 μm and α-Al_2O_3 (Baikowski grade SM8) with an average particle size ~0.6 μm. As-received powders were ball-milled in ethanol for 24 h. Electrophoretic deposition at a constant voltage was performed in a suspension flow-through deposition cell, where a supply system adds a second suspension to the circulating suspension in the mixing cell at a controlled rate. The process was performed in a way that would in theory lead to a symmetrical configuration of the layered system. The green bodies obtained with the EPD were sintered for 2 h at 1500 °C.

The resulting material was supplied in form of discs approximately 4 mm thick and with the diameter of 36 mm. The discs were formed by three layers with gradient transitions between them. The two outer layers consisted of a homogeneous mixture of 90% Al_2O_3 and 10% ZrO_2, the inner layer was a homogeneous mixture of 70% Al_2O_3 with 30% ZrO_2. A reference homogeneous material prepared by the same way with composition identical to that of the outer layers was also used.

3. Experimental methods

In order to observe the microstructure of all layers of the experimental material, the discs were cut perpendicularly with respect to the layers, the cross section surfaces were polished and thermally etched (1200 °C for 2 h at ambient air). The microstructure features were then studied using an SEM with an attached EDS unit.

Mechanical properties were investigated using indentation methods. Vickers hardness was measured across the polished surface of the specimen primarily in order to find the hardness profile. The indentations were carried out using a standard hardness tester and loadings of 3, 5, and 10 kg. In all cases the indents were aligned so that their diagonals and possible radial cracks were parallel and perpendicular to the composite layers. The sizes of the indents and the crack lengths were measured by an optical microscope. Indentation fracture toughness (K_{IC}) was calculated from the length of the cracks induced by the same indents using the Anstis et al.[5] formula:

$$K_{IC} = \eta \sqrt{\left(\frac{E}{H}\right)} \frac{F}{c^{3/2}}, \tag{1}$$

where η is a geometric factor estimated as 0.016, E the modulus of elasticity, H the hardness, F the indentation load, and c is the indentation radial crack half-length at the surface. Here, the c values were the lengths of the cracks parallel to the layers only, because these were not influenced by the in-plane residual stresses. From the length difference between these cracks (c, unstressed) and the cracks perpendicular to the layers (c_R, stressed) the in-plane residual stress (σ_R) can be calculated[6,7]

$$\sigma_R = \frac{K_{IC} - K_I}{Y c_R^{1/2}} = K_{IC} \frac{1 - (c/c_R)^{3/2}}{Y c_R^{1/2}} \quad \begin{matrix} > 0 \text{ tensile} \\ < 0 \text{ compressive} \end{matrix} \tag{2}$$

where K_I is the stress intensity factor for stressed crack, Y is the geometric factor ~1.26.

For the thermal shock study the indentation-quench method was chosen because of its simplicity and low cost. It is also a test that is rather low time consuming. According to Pettersson et al.[8] this method allows the use of one specimen throughout the test, whereas other methods, as, for example, the quench-strength method, require a whole set of specimens.

Nine indentations were made in the reference homogeneous specimen and 12 in the layered composite. Of the latter 12, 8 indents were introduced into the exterior layers and the remaining 4 indentations into the interior one. All indentations were made with a 3 kg load so that the pre-cracks would have approximately the same length. The lengths of the cracks were measured with the same equipment as in the hardness and fracture toughness tests. After that the specimens were heated up to a specified temperature and held there for 25–30 min in order to assure temperature uniformity before quenching. Then the specimens were rapidly immersed into a 20 °C water bath. After this the cycle was repeated; new measurements of the crack lengths were carried out, a heating up to a higher temperature was performed and finally the rapid cooling down into the water bath. The temperature used were: 150 °C (for the FGM only), 200, 250, 300, 350 and 400 °C.

4. Results and discussion

4.1. Microstructure

Low magnification SEM micrograph of a polished and thermally etched surface of the layered composite cross section (Fig. 1) shows the compositional changes in the different layers. Three thicker homogeneous layers separated by thinner compositionally graded intermediate layers can be observed. Fig. 2 shows SEM micrographs of a polished and thermally etched

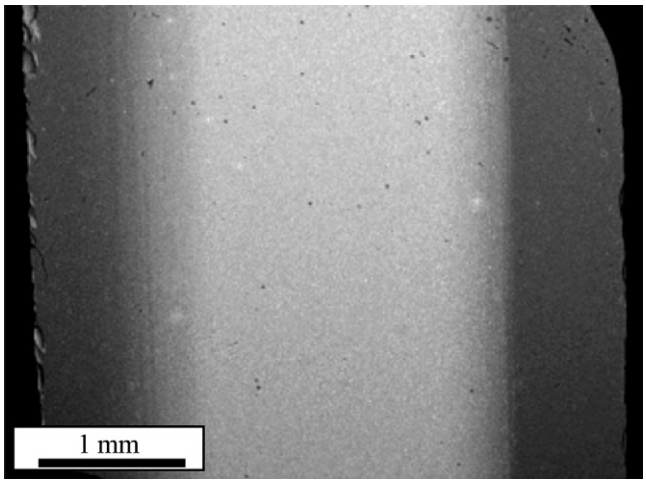

Fig. 1. Overall photograph showing the configuration of the homogeneous layers and gradient interfaces between them.

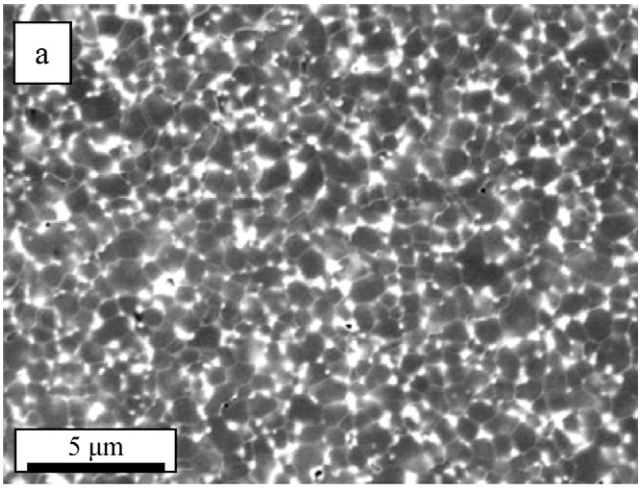

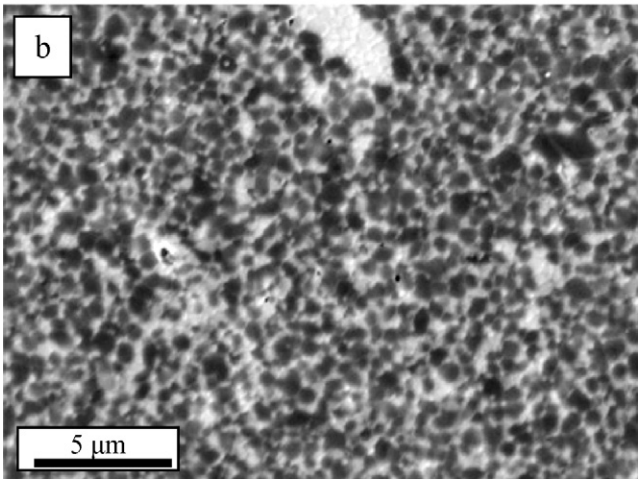

Fig. 2. Microstructures of the homogeneous layers of the FGM. (a) Outer layer; (b) central layer.

surface for each homogeneous layer, showing the grain sizes and the distribution of both principal phases. In the central layer (Fig. 2(b)), apart from homogeneously distributed zirconia (bright grains), occasionally zirconia agglomerates or grain chains can be seen. This can be deleterious for the mechanical stability of the composite, as we can expect higher local residual stresses in the vicinity of zirconia agglomerates. Also the martensitic transformation into monoclinic phase and the subsequent microcracking is more likely to occur in bigger grains. The SEM study also allowed measuring of the dimension of each layer, as they were not exactly known because of the nature of the EPD fabrication method. The outer homogeneous layers were 0.7 mm thick, the gradient ones 0.3 mm. The thickness of the inner homogeneous layer was 2 mm.

Generally, it can be seen, that the microstructure was well formed throughout the whole material. In the central layer it consisted of equiaxed alumina matrix grains with an average size of 0.5–0.9 μm and smaller homogeneously distributed zirconia grains with sizes between 0.2 and 0.4 μm. The zirconia grain clusters reached sizes up to 8 μm. The presence of zirconia effectively inhibited the alumina grain growth which can be demonstrated by the fact that in the outer layers (Fig. 2(a)) with lower zirconia contents the alumina grains had typically sizes from 0.7 up to 1.5 μm. The grain growth blocking is normally a desirable property since smaller grains imply better strength in the material, but in cases where one prioritises the creep resistance or fracture toughness, larger grains are eligible.

In all layers only very little porosity was observed, and even this seemed to be mostly due to the grain pull-out during polishing rather than a real feature of the microstructure.

4.2. Mechanical properties

The results of the hardness measurements are shown in Fig. 3. As expected the material closest to the edges was harder than the core material due to the higher content of alumina. This is a desired property, because a harder surface implies a better

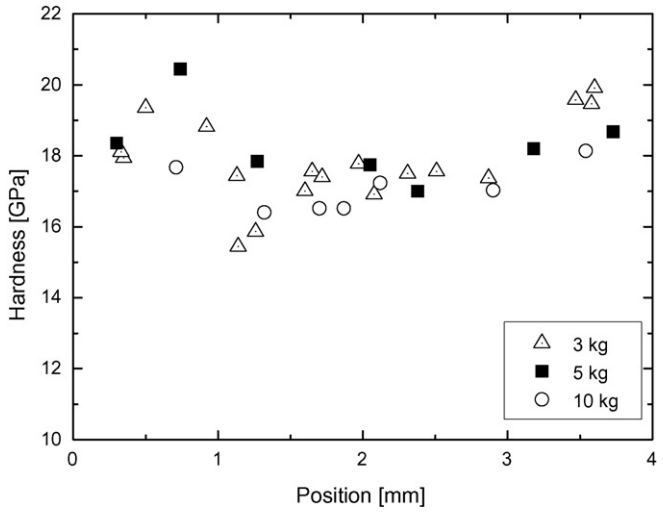

Fig. 3. Vickers hardness across the layered specimen measured using different indentation loads.

contact damage resistance. The highest hardness values measured were around 20 GPa, whereas the lowest values were around 16 GPa. These results are in a good agreement with literature data for technical ceramics.[9,10] Actually, the hardness of the exterior layers exhibits values more typical for monolithic alumina (18–20 GPa,[9,10] 17–18 GPa[11]) which can be attributed to the very dense, fine grained matrix, whose hardness had not been significantly decreased by the zirconia addition. The hardness of the central layer was comparable to that of Al_2O_3 + 15 vol.% ZrO_2 composite (15–16 GPa) studied by Casellas et al.,[11] a material with analogous compositional and microstructural characteristics. Again, considering higher zirconia contents, the present values are slightly higher, but the material in the mentioned paper[11] seems to contain more microdefects than the EPD composite studied in this work.

Fig. 4 shows the fracture toughness measurements for the graded material. As expected, the fracture toughness was higher in the central layer that contains 20 vol.% more of the tougher zirconia than the outer layers. The highest fracture toughness values were about 5.5–6 MPa $m^{1/2}$, whereas the lowest values were found to be 2–3 MPa $m^{1/2}$. The literature data for analogous homogeneous alumina/zirconia composites[11] range from 4.5 to ~5 MPa $m^{1/2}$ depending on the grain sizes. In this study the results tend to be a little lower, only the central part containing 30 vol.% ZrO_2 is tougher. However, this can be simply due to the fact that Casellas et al.[11] used a particularly calibrated value of the material constant η from the Eq. (1) which was about 50% higher than the standard value used in this work. If such higher value would have been used here, the K_{IC} values would be from 3 up to 9 MPa $m^{1/2}$, i.e. in a very good agreement with the literature.[11] Although no specific R-curve behaviour observation was performed (rising crack propagation resistance with crack growth), no particular trend in K_{IC} with respect to the indentation load was apparent. If some toughening takes place it is probable that the saturation crack length is rather short and that the effective K_{IC} stays the same for all indentation loads used in this test.

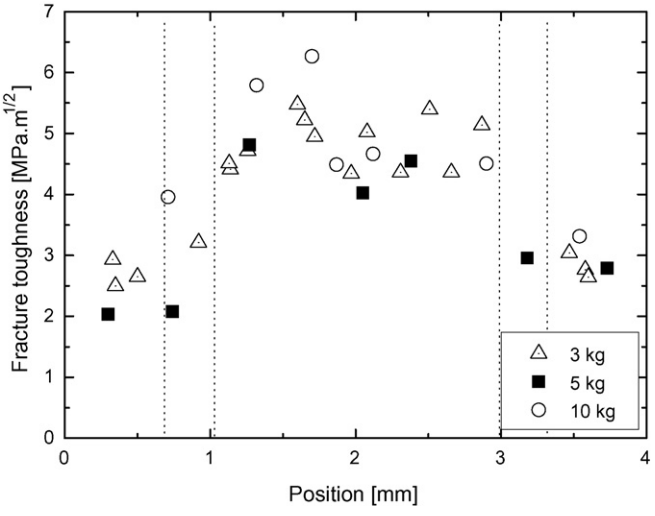

Fig. 4. Indentation fracture toughness. The dotted lines illustrate the layers of the material.

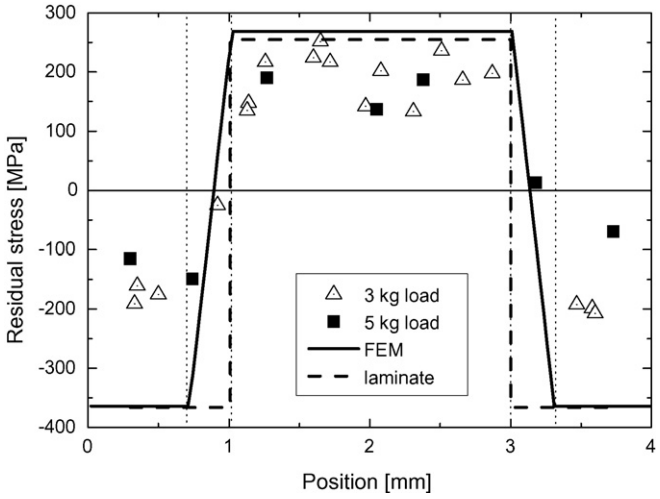

Fig. 5. Residual stresses measured by the indentation method compared to those calculated from thermal expansion coefficients using a finite element model and a simple symmetrical multilayered model.

The residual stresses calculated from the indentation cracks are shown in Fig. 5. The exterior layers were subjected to compressive stresses of about 200 MPa while in the interior layer tension with a maximum of about 240 MPa was found. No sharp stress changes exist and only low values of the residual stresses are found in the graded sections, showing that the theory of lowering stress concentrations by introducing graded transitions works very well.

In our preliminary experiments, when preparing the FGMs with compositional difference greater than 20% between the layers, we had observed, that it was impossible to produce them with the present geometry, because the samples disintegrated during cooling. Considering the present results, particularly the values of the residual tensile stress in the core layer, one can appreciate the reason. The tensile strength of high purity industrial alumina is typically 260–300 MPa, that of zirconia is ~250 MPa.[10] This means, that given the used layer thickness, the residual stresses within the tensile layer (up to 240 MPa) of the present experimental material with 20% difference of the ZrO_2 content approach the strength limit.

4.3. Finite element analysis

The residual stresses were also numerically modelled using finite element simulation (FEM) of sample cooling assuming only thermal contraction during cooling after sintering. The layer thicknesses were modelled according to the values measured by the SEM. A two dimensional model was created using rectangular elements varying Young's modulus and thermal expansion coefficient (α) along the specimen thickness. The Young's moduli and the thermal expansion coefficients were taken to be constant over the temperature range of cooling. Their values for the homogeneous layers are in Table 1.[12] All the values used in the model for the elements inside the gradient parts, which were not available in literature, were calculated from the properties in Table 1, using the linear rule of mixture, which can provide reasonably accurate estimates of the composite response in the

Table 1
Properties of the homogeneous layers[12]

	Inner layer 70% Al_2O_3 + 30% ZrO_2	Outer layer 90% Al_2O_3 + 10% ZrO_2
Thermal expansion coefficient	$10.20 \times 10^{-6}\,K^{-1}$	$8.99 \times 10^{-6}\,K^{-1}$
Elasticity modulus	318 GPa	373 GPa
Poisson's ratio	0.278	0.266

graded layer with small or negligible plastic strains.[13,14] The values of the residual stresses presented in Fig. 5 were estimated in the centre of the specimen along the direction normal to the layers. The specimen radius was large enough to avoid influence of the boundaries.

4.4. Laminate

Since the gradient layers were relatively thin when compared to the homogeneous ones, the material could be also approximated by a simple layered structure. Considering a system consisting of n layers a, each with thickness t_a, alternating with $(n-1)$ layers b, with thickness t_b, (Fig. 6) the residual stresses that arise due to thermal expansion coefficient mismatch only, can be easily calculated. In the absence of external load, the axial forces and moments acting on the layered system are in equilibrium. Pure temperature loading then leads to elastic stresses that are biaxial with the magnitudes[6,12,15]

$$\sigma_a = -\Delta\varepsilon \frac{E_a}{1-\nu_a}\left(1+\frac{nE_at_a}{(n-1)E_bt_b}\right)^{-1}$$
$$\sigma_b = \Delta\varepsilon \frac{E_b}{1-\nu_b}\left(1+\frac{(n-1)E_bt_b}{nE_at_a}\right)^{-1} \quad (3)$$

where the subscripts a and b denote the corresponding layers, ν the Poisson ratio, and $\Delta\varepsilon$ is the thermal strain mismatch which can be found taking into account the length change due to the cooling from the initial stress-free temperature (T_2) down to the room temperature (T_1):

$$\Delta\varepsilon = \varepsilon_a - \varepsilon_b = \int_{T_1}^{T_2} (\alpha_a - \alpha_b)\,dT \quad (4)$$

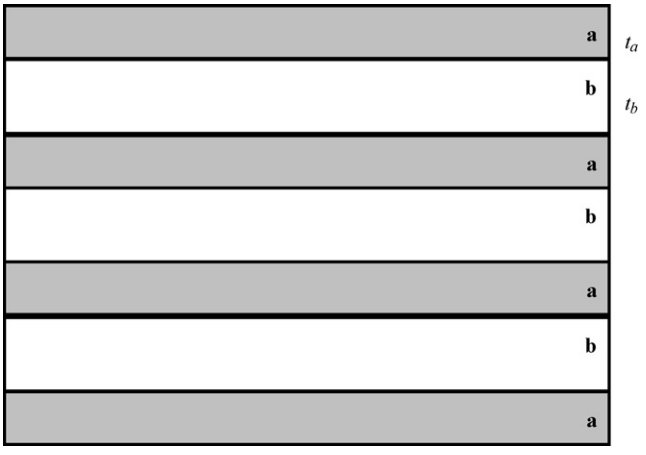

Fig. 6. Schematic drawing of a planar symmetrical multilayered laminate consisting of n layers a and $(n-1)$ layers b, with thickness t_a and t_b, respectively.

The calculated residual stresses are also shown in Fig. 5. Both models give very similar values with the highest tensile stress in the core layer being 269 MPa (FEM) or 255 MPa (laminate), respectively. The highest compressive stresses located in the exterior layers were 364 MPa (FEM) or 366 MPa (laminate), respectively. These values are higher than the measured ones. The reasons could include some residual stress relaxation, possibly by some deformation and/or transformation processes, or by porosity. However, using SEM only very little porosity was observed, and in our previous work[7] we had seen that the phase transformation in our materials was negligible. The discrepancy can be attributed to the fact that, during cooling, in the beginning the strain mismatch and possible arising stresses are accommodated by creep as long as the temperature is high enough and the joints between grains are not sufficiently strong.[16] Only below a certain, so-called "joining", temperature all components bind together and residual stresses appear. Consequently, it is possible, using the measured values of the residual stresses, to estimate this temperature by means of the Eqs. (3) and (4). Given the scatter of the data, in our case the "joining" temperature lay between 1200 and 1400 °C. The difference between the measured and the calculated values was largest in the outer layers which means that some additional stress relaxation took place there, most probably due to free surface effects.

4.5. Thermal shock

The Fig. 7(a–c) show the results of the thermal shock tests. The maximum crack length marked out is 300 μm. Larger crack lengths correspond to unstable cracking (cracking to the edges or into other indentations). For better visibility in the photographs, the surfaces were after the tests impregnated with a penetrating dye. Again, the cracks produced in directions parallel and transversal with respect to the layers did not have the same lengths directly after the indentations, due to the residual stresses.

After quenching, in the interior layer (residual tension) the transversal cracks had grown about 20–30% already at temperature differences of $\Delta T = 180\,°C$, and at the temperature difference 230 °C all but one crack had grown uncontrollably. At the same temperature difference, the parallel cracks were rather stable, and started to grow unstably only at the temperature difference of 330 °C. The transversal cracks ceased to propagate when they had reached the exterior (compressive) layers (Fig. 8(a)).

In the exterior layers the inverse phenomena can be seen due to the inverse stresses. The cracks began to propagate in the parallel direction already at low temperature differences whereas the transversal cracks were rather stable and did not propagate much at the same temperatures differences. It was first at $\Delta T = 280\,°C$ that the transversal cracks started to propagate of considerable proportions and at $\Delta T = 330\,°C$ only 60% of the cracks had grown uncontrollably.

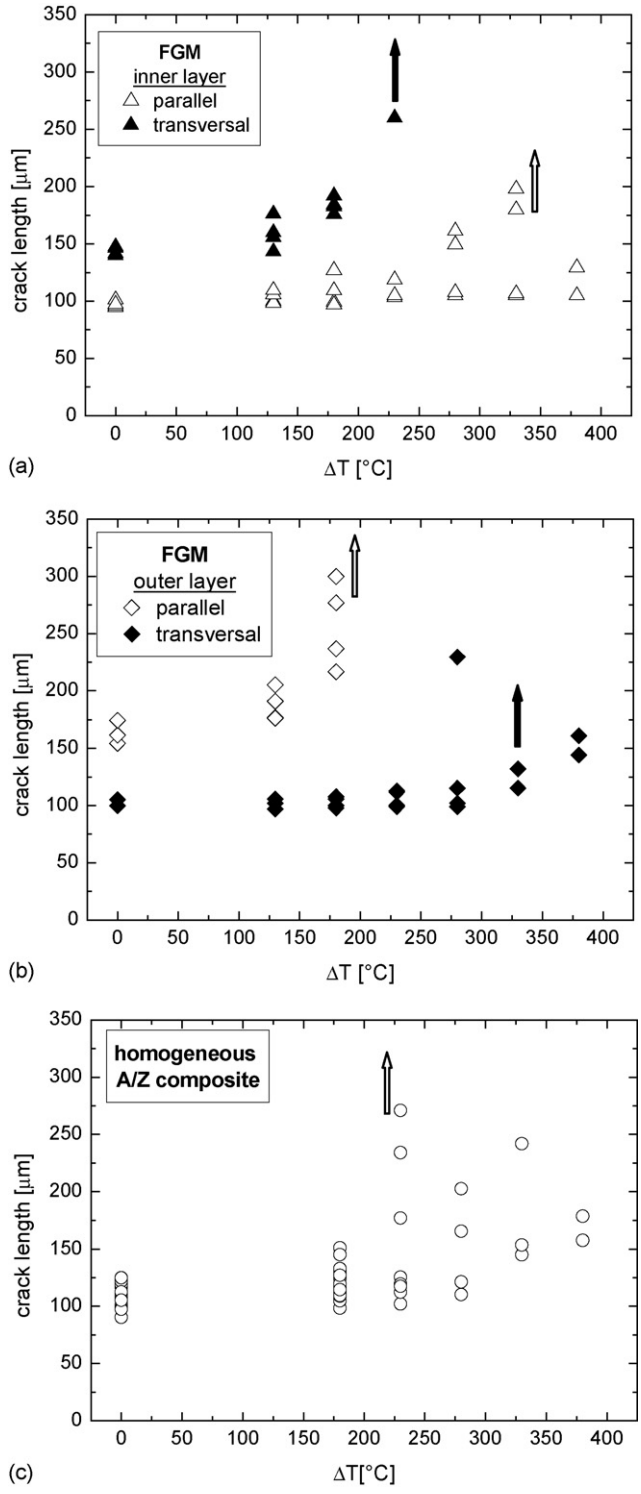

Fig. 7. Crack propagation at thermal shock tests. (a) FGM, inner layer; (b) FGM, outer layer; (c) homogeneous composite. The critical temperature differences at which unstable cracking begins are marked by arrows.

For the homogeneous specimen the crack propagation in parallel and transversal directions did not differ since no macroscopic residual stresses existed there. Already after the first quench at the temperature difference of 180 °C the cracks had grown up to 50%. After the quench of 230 °C more than half of the cracks had either grown more than 100% or they had grown

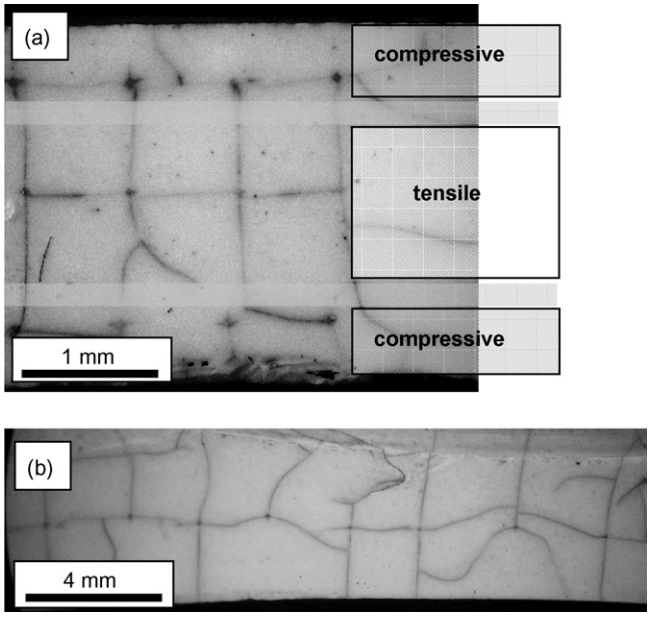

Fig. 8. The experimental materials after the thermal shock tests. (a) FGM, limited growth of the transversal cracks within the outer (compressive) layers; (b) homogeneous composite.

uncontrollably and connected themselves with other cracks. At the temperature difference of 280 °C more than 90% of the introduced cracks had grown uncontrollably. As it can be seen in the Fig. 8(b) the cracks did not stop before the edges.

The graded material had a very good ability to stop cracks propagating from the interior layers of the specimen before they reached the edges, and to resist the transversal crack growth. This property, due to compression stresses, decreases the chances of complete breakdown of the material considerably.

5. Conclusions

An experimental alumina/zirconia planar FGM prepared by EPD has been studied. The material had in all layers a high quality fine grained microstructure with very little overall porosity and uniformly distributed ZrO_2 within the homogeneous layers. The zirconia grains effectively hindered the growth of alumina matrix grains.

The hardness, fracture toughness, and residual stresses were measured by indentation methods on the cross section of the sample. Their changes with respect to the compositional profile were identified. The material exhibited excellent hardness in the exterior layers, comparable to that of pure alumina.

The measured values of the residual stresses were compared to those calculated by a finite element simulation and by a simple laminate model. Both models, mutually in agreement, tend to overestimate the results. This has been attributed to a slightly lower actual joining temperature and to free surface effect.

Thermal shock tests, studied by indentation-quench method, show highly enhanced resistance of the FGM against transversal propagation of surface cracks, which in real applications might form by impacts, wear or other contact mechanisms during the use, into the bulk. No observable transversal crack originated

from the side surfaces of the specimen, even though these were not polished. This can be contrasted to the crack propagation in the homogeneous material, where no preferential directions for crack growth and no crack arresting were observed.

Acknowledgements

The work was supported by the Ministry of Science and Technology of Spain through the "Ramón y Cajal Programme". The experiments were performed in the framework of the EU Training Network "SICMAC" (contract HPRN-CT-2002-00203), with financial support of the Marie Curie Reintegration Grant (contract MERG-CT-2004-005807).

References

1. Lugovy, M., Orlovskaya, N., Berroth, K. and Kuebler, J., Macrostructural engineering of ceramic-matrix layered composites. *Compos Sci Technol*, 1999, **59**, 1429–1437.
2. Suresh, S. and Mortensen, A., *Fundamentals of functionally graded materials*. ASM International and The Institute of Materials, Cambridge, 1995.
3. Suresh, S., Modeling and design of multi-layered and graded materials. *Prog Mater Sci*, 1997, **42**, 243–251.
4. Vleugels, J., Anné, G., Put, S. and Van Der Biest, O., *Thick plate-shaped Al_2O_3/ZrO_2 composites with continuous gradient processed by electrophoretic deposition. Functionally graded materials VII*. Trans Tech Publications, Switzerland, 2003, pp. 171–176.
5. Anstis, G. R., Chantikul, P., Lawn, B. R. and Marshall, D. B., A critical evaluation of indentation techniques for measuring fracture toughness: I. Direct crack measurements. *J Am Ceram Soc*, 1981, **64**, 533–538.
6. Green, D. J., Cai, P. Z. and Messing, G. L., Residual stresses in alumina-zirconia laminates. *J Eur Ceram Soc*, 1999, **19**, 2511–2517.
7. Hvizdoš, P., Calderón Moreno, J. M., Očenášek, J., Ceseracciu, L. and Anné, G., Mechanical properties of alumina/zirconia functionally graded material prepared by electrophoretic deposition. *Key Eng Mater*, 2005, **290**, 332–335.
8. Pettersson, P., Johnsson, M. and Shen, Z., Parameters for measuring the thermal shock of ceramic materials with an indentation-quench method. *J Eur Ceram Soc*, 2002, **22**, 1883–1889.
9. Morrell, R., *Handbook of properties of technical and engineering ceramics, Part 1*. HMSO, London, 1985.
10. Ferro-Ceramic Grinding, Inc., http://www.ferroceramic.com/.
11. Casellas, D., Nagl, M. M., Llanes, L. and Anglada, A., Fracture toughness of alumina and ZTA ceramics: microstructural coarsening effects. *J Mater Process Technol*, 2003, **143–144**, 148–152.
12. Sbaizero, O. and Lucchini, E., Influence of residual stresses on the mechanical properties of a layered ceramic composite. *J Eur Ceram Soc*, 1996, **16**, 813–818.
13. Giannakopoulos, A. E., Suresh, S., Finot, M. and Olsson, M., Elastoplastic analysis of thermal cycling: layered materials with compositional gradients. *Acta Metall Mater*, 1995, **43**, 1335–1354.
14. Finot, M., Suresh, S., Bull, C. and Sampath, S., Curvature changes during thermal cycling of a compositionally graded Ni-Al_2O_3 multi-layered material. *Mater Sci Eng A*, 1996, **205**, 59–71.
15. Hvizdoš, P. *et al.*, Micostructure and mechanical properties of an alumina/zirconia FGM prepared by EPD. In *Proceedings of Deformation and Fracture in Structural PM Materials*, ed. Ľ. Parilák and H. Danninger. Stará Lesná, Slovakia, September 2005, pp. 266–273.
16. Lugovy, M., Slyunyayev, V., Orlovskaya, N., Blugan, G., Kuebler, J. and Lewis, M., Apparent fracture toughness of Si3N4-based laminates with residual compressive or tensile stress in surface layers. *Acta Mater*, 2005, **53**, 289–296.